HHS Public Access

Author manuscript

Arch Biochem Biophys. Author manuscript; available in PMC 2017 July 01.

Published in final edited form as:

Arch Biochem Biophys. 2016 July 1; 601: 32–41. doi:10.1016/j.abb.2016.03.012.

Liver Kinase B 1 Complex Acts as a Novel Modifier of Myofilament Function and Localizes to the Z-Disk in Cardiac Myocytes

Samantha M. Behunin, **Marissa A. Lopez-Pier**, **Rachel M. Mayfield**, **Christiane A. Danilo**, **Yulia Lipovka**, **Camille Birch**, and **Sarah Lehman**

Department of Physiology, Sarver Molecular Cardiovascular Research Program, University of Arizona, 1501 N. Campbell Ave., Tucson, AZ, 85724, United States

Jil C. Tardiff[1], **Carol C. Gregorio**[1], and **John P. Konhilas**[*]

[1]Department of Molecular and Cellular Biology, Cellular and Molecular Medicine, Sarver Molecular Cardiovascular Research Program, University of Arizona, 1501 N. Campbell Ave., Tucson, AZ, 85724, United States

Abstract

Contractile perturbations downstream of Ca^{2+} binding to troponin C, the so-called sarcomere-controlled mechanisms, represent the earliest indicators of energy remodeling in the diseased heart [1]. Central to cellular energy "sensing" is the adenosine monophosphate-activated kinase (AMPK) pathway, which is known to directly target myofilament proteins and alter contractility [2-6]. We previously showed that the upstream AMPK kinase, LKB1/MO25/STRAD, impacts myofilament function independently of AMPK [5]. Therefore, we hypothesized that the LKB1 complex associated with myofilament proteins and that alterations in energy signaling modulated targeting or localization of the LKB1 complex to the myofilament. Using an integrated strategy of myofilament mechanics, immunoblot analysis, co-immunoprecipitation, mass spectroscopy, and immunofluorescence, we showed that 1) LKB1 and MO25 associated with myofibrillar proteins, 2) cellular energy stress re-distributed AMPK/LKB1 complex proteins within the sarcomere, and 3) the LKB1 complex localized to the Z-Disk and interacted with cytoskeletal and energy-regulating proteins, including vinculin and ATP Synthase (Complex V). These data represent a novel role for LKB1 complex proteins in myofilament function and myocellular "energy" sensing in the heart.

Graphical abstract

Graphic representation of hypothesis and results. We tested the hypothesis that the LKB1 complex associated with myofilament proteins in the sarcomere and altered this association with energy

[*]To whom correspondence should be addressed: John P. Konhilas, PhD, University of Arizona, Department of Physiology, Sarver Molecular Cardiovascular Research Program, Medical Research Building, room 320, Tucson, AZ 85721-0241, Tel: (520)-626-6578, Fax: (520)-626-7600, konhilas@arizona.edu.

stress. In general, creatine kinase (**CK**) and adenylate kinase (**AK**) balance the available AT =P for use by the contractile proteins, specifically myosin. Pathological energy stress from FHC or CVD elevates myofibrillar AMP that recruits LKB1 and AMPK complex proteins to myofibrils. LKB1 activates AMPK in the presence of elevated AMP, which directly impacts myofilament function.

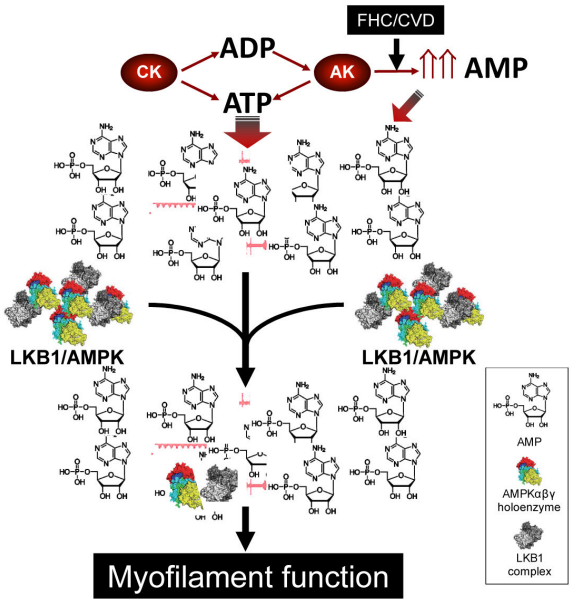

Keywords

Liver Kinase B1 (LKB1); Z-disk; myofibril; myofilament; contractility; vinculin

Introduction

The cardiac myocyte undergoes extensive metabolic and energetic remodeling during the progression of heart disease. Contractile perturbations downstream of Ca^{2+} binding to troponin C, the so-called sarcomere-controlled mechanisms, may represent the earliest indicators of this remodeling [1]. Accordingly, the *dynamics* of cardiac contraction and relaxation during cardiovascular disease (CVD) are governed by downstream mechanisms, particularly the *kinetics* and *energetics* of the cross-bridge cycle [7]. Energy disturbance from CVD initiates cellular signaling cascades that become integrated with cross-bridge kinetics at the level of the contractile proteins, or *myofilament* [1, 8].

The failing heart has long been characterized as energy starved [9-11] and central to this energetic remodeling is an alteration in the production, use and delivery of adenosine triphosphate (ATP). In fact, disturbances in the creatine kinase(CK)/adenylate kinase(AK) phosphotransfer system are observed early in CVD and are stronger predictors of heart failure mortality than functional status [12]. Given the physical barriers to rapid diffusion within the myocyte, physical association of CK, AK, and other key enzymes in the phosphotransferase system optimizes efficient transfer of phosphoryl groups to adenosine diphosphate (ADP) [13]. These phosphotransfer components exist in discrete microdomains

and are localized to sarcomeric myofibrils acting as hubs for energy "sensing" [14, 15]. More importantly, these phosphotransferase enzymes display remarkable plasticity in function and compartmentation during energy stress [16]. Perturbations in the balance of ATP supply and demand imbalance commonly occur during CVD. During this imbalance, AK amplifies the amount of adenosine monophosphate (AMP) within these microdomains while it attempts to preserve ATP levels for contraction [17].

Central to AMP sensing is the adenosine monophosphate-activated kinase (AMPK) pathway, which also displays remarkable plasticity during CVD. AMPK is a phylogenetically conserved heterotrimeric complex consisting of a catalytic α subunit and regulatory β and γ subunits [18]. An increase in myocellular AMP, as occurs with cardiac disease, allosterically activates AMPK and permits phosphorylation of the α catalytic subunit at Thr^{172} by the upstream Liver Kinase B1 (LKB1) kinase complex [19-21]. LKB1 acts in concert with MO25 (mouse protein 25) and STRAD (ste-related adaptor protein) to phosphorylate AMPK potentiating its activity and promoting ATP producing pathways while inhibiting ATP consuming pathways [20, 21]. In addition, AMPK targets Ser^{150} of Troponin I ($p\text{-}cTnI_{ser150}$) and subsequently increases myofilament sensitivity to Ca^{2+} [2-6].

Evidence exists to support the idea that AMP binding to AMPK initiates assembly of an activating complex that brings LKB1/MO25/STRAD into close association with AMPK allowing phosphorylation of Thr^{172} on AMPKα by LKB1/MO25/STRAD [22]. Once the components of the upstream kinase complex are bound together LKB1/MO25/STRAD becomes constitutively active [23]. Therefore, controlling when and where the subunits of the LKB1/MO25/STRAD complex are expressed is key to regulating its function. Indeed, there have been some studies in adipocytes and skeletal muscle that suggest posttranslational modification of LKB1 leads to alterations in subcellular localization [24, 25]. Therefore, the AMPK/LKB1 signaling pathway is subject to regulation by not only AMP pools but also to alterations in the subcellular association of AMPK and LKB1/MO25/STRAD. This mechanism of regulation is similar to the phosphotransferase CK system, which is a paradigm of subcellular localized enzyme organization [16, 26]. For this reason, we propose that AMPK/LKB1 complex proteins act as a nodal point for sensing changes in CK and AK activity through changes in the ATP pool and directly tuning myofilament function to the energetic demand through post-translational modifications.

We recently presented data illustrating how differing molar ratios of AMPK and LKB1/MO25/STRAD impact myofilament function. In addition, we provided the first evidence that the upstream LKB1/MO25/STRAD complex had the ability to modify contractile function independently of AMPK [5]. For these reasons we hypothesized that the LKB1 complex associates with myofilament proteins and that alterations in energy signaling modulate targeting or localization of the LKB1 complex to the myofilament. To that end we have found that 1) myofibrillar proteins retained or bound LKB1 and MO25; 2) cardiovascular energy stress re-distributed LKB1 and MO25 localization within myofibrillar proteins; 3) LKB1 complex proteins robustly localized at the Z-Disk.

Materials and Methods

Animal Subjects

Animal models included male Sprague-Dawley rats, aged two months; four month old male R403Q transgenic mice; and four month old male c57/bl6 mice. All experiments were performed using protocols that adhered to guidelines and approved by the Institutional Animal Care and Use Committee at the University of Arizona and to NIH guidelines for care and use of laboratory animals.

Isolation and Perfusion with 5-Aminoimidazole-4-Carboxamide Ribonucleotide

Rats were anesthetized with isoflurane and their hearts rapidly excised. Control hearts were then retrogradely perfused through the aortic stump with a Krebs-Henseleit solution (NaCl 118.5 mmol/L, KCl 5 mmol/L, $MgSO_4$ 1.2 mmol/L, NaH_2PO_4 2 mmol/L, D-(+)-glucose 10 mmol/L, $NaHCO_3$ 25 mmol/L, $CaCl_2$ 0.2 mmol/L, and 2,3-Butanedione monoxime (20 mmol/L) [27]. For separate 5-Aminoimidazole-4-carboxamide ribonucleotide (AICAR) treatment, a modified Krebs-Henseleit solution containing 2mM AICAR was used for perfusion. All hearts were retrogradely perfused for 30 minutes. Following perfusion, hearts were flash frozen and stored for proteomic analysis at −80°C.

Trabecular Isolation and Treatment with LKB1/MO25/STRAD

Sprague-Dawley rats were anesthetized with isoflurane and their hearts rapidly excised. Hearts were then retrogradely perfused with a modified Krebs-Henseleit solution. Thin, even, free standing trabeculae were isolated from the right ventricular wall, as well as left ventricular papillaries. Following isolation, trabeculae and cut papillaries were transferred to an ice-cold relax solution (Na_2ATP 5.95mmol/L, $MgCl_2$ 6.41mmol/L, EGTA10mmol/L, K^+Propionate 50.25mmol/L, phosphocreatine 10mmol/L, N,N-bis(2-hydroxyethyl)-2-aminoethanesulfonic acid (BES) 100 mmol/L, phenylmethylsulfonyl fluoride (PMSF) 0.1mmol/L, dithiothreitol (DTT) 1mmol/L, 50 U/mL creatine phosphokinase, and protease inhibitor cocktail (Sigma) 4μL cocktail/ml solution) containing 1% Trition X-100 for overnight demembranation at 4°C [2, 27]. Following demembranation, 50nM of active recombinant LKB1/Mo25/STRAD (Millipore) was added to demembranated trabeculae for 30 minutes at 30°C. After incubation, fibers were washed (15 min; repeated three times) with standard relaxing buffer on ice. The Ca^{2+}-Force relationship was then measured for each fiber, followed by flash freezing and storage at −80°C. The treatment/incubation prot ocol is summarized in **Figure 1**.

Experimental Apparatus and Protocol

The experimental apparatus for mechanical measurements of cardiac trabeculae was similar to that described previously [27]. The fiber was attached to the apparatus via aluminum T-clips to stainless steel hooks that extended from a high-speed servomotor (Aurora Scientific model 315C) and a modified silicon strain gauge force transducer (model AE801, Kronex, CA), both of which were attached to X-Y-Z manipulators mounted on a temperature controlled stage (15 ± 0.1 C). Force was digitally converted with an A/D converter and custom software (LabVIEW, National Instruments; Austin, Texas) for off-line analysis.

Ca^{2+}-sensitivity of tension development as a function of sarcomere length was determined by activating the muscle during a series of pre-activating-activating-relaxation cycles using a range of free [Ca^{2+}] in the activating solutions (**Table 1**) selected in random order [27].

Sarcomere length (SL) was set at 2.2μm determined from the first order He-Ne laser light diffraction band monitored by a 2048 pixel high speed linear CCD sensor (Dexela Ltd., London, UK) and adjusted to maintain constant SL throughout contraction. Fibers were allowed to reach steady state tension and then rapidly slackened by 20% of total fiber length. The difference between steady state tension and slacked tension determined total tension. Active tension at each [Ca^{2+}] is the difference between total tension and relaxed, passive tension. For all experiments, fibers that did not retain 85% of initial maximal tension or a detectable diffraction pattern were discarded. Given these stringent criteria, yields for mechanical experiments were approximately 10%. At the completion of the experimental protocol, tissue was flash frozen in liquid nitrogen and stored at −80°C for proteomic analysis.

Skinned Myocyte Preparation

Frozen tissue (twenty mg) was homogenized into relax for 10-15s using a drill press. After homogenization, sample was gently spun and supernate removed. Relax containing 0.3% Triton-X100 was added to the pellet and incubated on ice for 5 minutes. Following skinning with 0.3% TritonX-100, sample was gently spun and supernate was removed. Sample was then resuspended in relax and allowed to pellet on ice, and the supernate was removed. 100uL of solubilization buffer (8M Urea, 2M Thiourea, DTT, SDS) was added to sample and heated for 10 minutes at 60°C. Samples were then spun, frozen, and stored at −80°C .

Myofibrillar Isolation

Myofibrillar proteins from frozen tissue were isolated as detailed previously [28]. Briefly, frozen tissue was transferred to a dounce homogenizer containing a relaxing buffer (75mM KCl, 10mM imidazole (pH 7.2), 2mM $MgCl_2$, 2mM EDTA, amd 1mM NaN_3) and 1% Triton X-100 and homogenized. The sample was then spun down and the supernatant was removed. Samples were then washed in a relaxing buffer without Trition X-100 to remove all detergent. After washing, UTC buffer (8M Urea, 2M Thiourea, 4% CHAPS) was then added to the sample based upon a 1:20 (W/V) ratio of sample to UTC. Samples were transferred back to the dounce and homogenized. Following homogenization, samples were placed on an orbital shaker for 30 minutes and then placed in a water bath sonicator for 10 minutes. Samples were then spun to obtain a clarified soluble sample. Aliquots were flash frozen in liquid nitrogen and stored at −80°C.

Immunoblot

Samples were separated using SDS-PAGE (12% acrylamide). Following electrophoresis, proteins were transferred to a polyvinylidene fluoride (PVDF) membrane using the Trans-Blot® SD Semi-Dry Transfer Cell (BioRad). Following transfer, total protein was measured with Ponceaus S stain (Sigma). Total protein optical density from the Ponceaus S stain was measured with LabImage 1D software. There was no difference in loading between any group ($P>0.05$). Antibodies were used to probe for LKB1 (1:1000, Cell Signaling), Mo25

(1:2000, Cell Signaling), phospho-Thr^{172}AMPKα (1:1000, Cell Signaling), and AMPKα (1:1000, Cell Signaling). Protein optical densities were quantified using LabImage 1D software.

All immunoblot analysis was performed from the semi-quantitation of individual blots and was not compared across blots according to accepted guidelines. Some immunoblot images of a given target were cropped from the same blot in order to conserve figure space and limit redundancy.

Co-Immunoprecipitation and Mass Spectrometry

Co-immunoprecipitation was performed using a kit from Thermo-Scientific according to manufacturer's instructions. Antibodies for Mo25 (Cell Signaling) were immobilized on the column. Following anti-Mo25 immobilization, demembranated heart tissue treated with active recombinant LKB1/Mo25/STRAD (50nM LKB1, 30 minutes) as well as tissue from AICAR treated hearts were added to the column and incubated overnight at 4°C. Columns were then washed, and the Co-IPs were eluted. Eluted samples were then prepared for SDS-PAGE by adding solubilization buffer and heated for 5 min at 90°C.

Following SDS-PAGE, silver stain was performed to visualize proteins associating with Mo25. Identity of bands, or candidates for MO25 binding, were analyzed with LC-MS/MS by the Arizona Proteomics Consortium. Charge state deconvolution and deisotoping were not performed. All MS/MS samples were analyzed using Sequest (Thermo Fisher Scientific, San Jose, CA, USA; version 1.3.0.339).

Criteria for protein identification

Scaffold (version Scaffold_4.4.1.1, Proteome Software Inc., Portland, OR) was used to validate MS/MS based peptide and protein identifications. Peptide identifications were accepted if they could be established at greater than 10.0% probability to achieve an FDR less than 0.1% by the Scaffold Local FDR algorithm. Protein identifications were accepted if they could be established at greater than 99.0% probability and contained at least 2 identified peptides. Protein probabilities were assigned by the Protein Prophet algorithm [29]. Proteins that contained similar peptides and could not be differentiated based on MS/MS analysis alone were grouped to satisfy the principles of parsimony. Proteins sharing significant peptide evidence were grouped into clusters.

Mouse Myocyte Isolation and Treatment with AICAR

Male (4 month) c57/bl6 mice were anesthetized with isoflurane and their hearts rapidly excised. Myocytes were isolated from enzymatically digested hearts according to previously published methods [2]. Cardiomyocytes obtained after enzymatic digestion were cultured on 18×18 coverslips (Fisherbrand cat#12-542A) coated with 1:20 dilution of Matrigel (Corning GFR #354230) in DMEM (Gibco #11885) with 1% Pen/Strep and 10% heat inactivated FBS (Gibco #16141-079) for approximately 1 to 2hrs at 37°C. Isolated myocytes were then treated for 20 minutes with 2mM 5-aminoimidazole-4-carboxamide ribonucleotide (AICAR). Post-treatment, the cells were washed 3x with 1x PBS. 1mL of 1x relax solution with 4mM ATP was added to the coverslips and rocked for fifteen minutes at room

temperature. The relax solution was removed and cardiomyocytes were fixed with 1mL of 2%formaldehyde/1x relax with 4mM ATP. Fixed cardiomyocytes were stored at 4°C for subsequent im munofluorescent staining.

Immunofluorescent Staining Intact Cardiomyocytes

Fixed mouse cardiomyocytes were permeablized in 0.2% Triton X-100/PBS for twenty minutes at room temperature. Next, cardiomyocytes were treated with 1mg/ml solution of Sodium Borohydride dissolved in 1x PBS for 4 mins, repeated twice. Cardiomyocytes were then rinsed with 1x TBS with 1% Tween (TBS-T) 3x for five minutes each. Once all residual sodium borohydride had been removed, cardiomyocytes underwent a 1% SDS Antigen Retrieval for five minutes then washed with 1x TBS-T 3x for 5mins each. Cardiomyocytes were blocked with 2% BSA plus 1% normal donkey serum/PBS for 1 hour at room temperature and incubated overnight at 4°C with mouse monoclonal anti- α-actinin (1:200, EA-53, Sigma) and polycolonal anti-LKB1 (1:100, 05-832, EMD Millipore) or monoclonal anti-sarcomeric- α-actinin (1:100, ab68167, abcam) and monoclonal anti-M025 (1:100, ab51132, Abcam).Sections were then washed with 1X TBST-T for twenty minutes, and incubated with secondary antibodies/TBS-T for 1.5 hours. Secondary antibodies (Invitrogen) included Alexa Fluor 488-conjugated goat anti-mouse IgG (1:1,000) and Alexa Fluor 350-conjugated goat anti-mouse IgG (1:200) for the staining of α-actinin and anti-LKB1. Secondaries used for monoclonal anti-sarcomeric- α-actinin and monoclonal anti-Mo25 were Alexa Fluor 350 anti-rabbit IgG (1:200, A21049, Invitrogen) and Alexa Fluor 488 goat anti-rabbit IgG (1:500, A11034, Molecular Probes) respectively. Texas-Red- or Alexa Fluor 488-conjugated phalloidin (1:50) was used to stain F-actin. Sections were washed with TBS-T for twenty minutes then mounted onto slides with Aqua Poly/Mount (Polysciences Inc.). Images were captured using a Deltavision RT system (Applied Precision) with a 100× NA 1.3 objective, and a charge-coupled device camera (CoolSNAP HQ; Photometrics). Images were deconvolved using SoftWoRx software and processed using Photoshop CS (Adobe).

Immunofluorescent Staining Skinned Cardiomyocytes

Skinned rat cardiomyocytes obtained from frozen perfused and AICAR perfused hearts were fixed for 2hrs with a 4% formaldehyde/PBS solution in suspension using 1.5mL eppendorf tube at 4°C using a spinning end over end rocker to avoid clumping of cells. After fixation the cells were then quenched to remove any of the leftover aldehyde groups in the fixative with 20mM NH_4Cl for 5mins. The adult mouse cardiomyocytes were permeablized in 0.2% Triton X-100/PBS for 20 min at room temperature. The cells were then washed 2x times with 500uL of ice-cold TBST-T. The cell suspension underwent a 1%SDS Antigen Retrieval for five minutes then washed with 1x TBS-T 3x for five minutes. Incubation of primary and secondary antibodies as well as imaging was done as described above.

Data and Statistical Analysis

Tension in submaximally activating solutions was expressed as fractions (P/P_0) of the maximum tension (P_0) at the same sarcomere length. The P_0 value used to normalize submaximal tension was obtained by linear interpolation between successive maximal activations. Each individual Ca^{2+}-tension relationship was fit to a modified Hill equation where $P_{rel} = [Ca^{2+}]^n/(EC_{50} + [Ca^{2+}]^n)$, P_{rel} = relative tension, $EC_{50} = [Ca^{2+}]$, or pCa_{50}

(−log [EC_{50}]) at which tension is half-maximal, n = slope of the Ca^{2+}-tension relationship (Hill coefficient). Tension redevelopment after the release and restretch protocol (**k**tr) was fit by linear or exponential least squares model of the **k**tr-P/P_0 relationship. Quantitation of Western blot analysis represents comparisons between AICAR-treated or FHC hearts and respective controls by a Student T-test. Results are presented as mean ± SEM. Student's-t test was used to determine differences in means. P values less than 0.05 were considered significant.

Results

LKB1 complex blunts contractile function

The function and regulation of the LKB1 complex in the majority of tissues are not well known, particularly in the heart. In our previous study, treatment of demembranated rat cardiac trabeculae with increasing amounts of LKB1 complex relative to AMPK decreases Ca^{2+}-sensitivity of tension and blunts maximum tension development [5]. Therefore, the first series of experiments were to validate our previous work. Consequently, we assessed Ca^{2+}-sensitivity of tension, maximum tension, and the rate constant for tension redevelopment in demembranated cardiac trabeculae incubated with LKB1 complex. Consistent with our previous data [5], fibers treated with the LKB1 complex exhibited a significant decrease in Ca^{2+}-sensitivity of tension (**Figure 2A**). In addition, tension at maximum Ca^{2+} (maximum tension) was significantly blunted in cardiac trabeculae treated with LKB1 complex proteins (**Figure 2B; Table 1**).

In light of this robust desensitization to Ca^{2+} and loss of maximum tension, we wished to determine how LKB1 complex treatment impacted cross-bridge kinetics. The rate constant for tension redevelopment ($\boldsymbol{k}_{tr}$) measures the sum of the apparent rates with which actin-myosin cross-bridges enter and leave tension generating states [30]. There were no differences in maximal, or Ca^{2+} saturating, $\boldsymbol{k}_{tr}$ between the treatment groups. As $\boldsymbol{k}_{tr}$ is dependent on levels of activating Ca^{2+} and strongly bound cross-bridges, $\boldsymbol{k}_{tr}$ was determined over a range of submaximal activating Ca^{2+}, plotted against relative tension (P/P_0) and fit by linear or curvilinear (exponential) least squares model. **Figure 2C** and **Figure 2D** shows the summed representations of curve fits to the relationship of P/P_0 to $\boldsymbol{k}_{tr}$. Despite a decrease in Ca^{2+} sensitivity, LKB1 complex treated fibers displayed no difference in the relative tension-$\boldsymbol{k}_{tr}$ linear relationship compared to untreated fibers, whether fit by a linear [30] or a curvilinear model [5].

LKB1 complex associates with myofibrillar proteins

Although our previous work shows that LKB1 complex treatment of demembranated cardiac tissue increases total phosphorylation of myosin binding protein C (MBPC), this is not causative to the decrease in Ca^{2+} sensitivity of tension development. The reason is that selective phosphorylation MBPC at serine 282 is accompanied by a significant reduction in Ca^{2+} sensitivity and a significant acceleration of cross-bridge cycling kinetics [31], different from what we find here. We obtained some insight as to this mechanism when we discovered that *demembranated* trabeculae treated with the LKB1 complex (recombinant GST-LKB1/MO25/STRAD) retain the complex even after a stringent washout protocol to remove excess

kinase complex (**Figure 3**). Demembranation removes all membrane-bound organelles, leaving primarily components involved in “downstream” regulation of contraction including ultrastructural and contractile myofilament proteins. The implication is a robust association of the LKB1 complex with sarcomeric proteins.

It is not surprising that exogenously added proteins display a strong interaction with myofilament proteins that remain after some period of incubation. Therefore, it is important to answer the question as to whether there is endogenous association between proteins of the AMPK/LKB1 signaling axis and the myofilament. The presence of recombinant GST-LKB1/MO25/STRAD protein complex is 2-3 fold higher than endogenous AMPK/LKB1 complex proteins and has a slightly higher kDa due to the GST tag and cannot be visualized in the same immunoblot. Therefore, endogenous association was confirmed in a separate immunoblot (Western) analysis of demembranated cardiac tissue with antibodies specific for AMPK, $pAMPK_{thr172}$, LKB1, and MO25 (see **Figure 6**). This presents the first evidence that each component of the AMPK signaling network associated and/or localized to myofilament proteins.

LKB1 Complex Localizes to the Z-Disk of the Sarcomere

The suggestion from our studies is that AMPK, LKB1, and MO25 localize to the myofilaments. Using an immunohistochemistry approach, we present novel data that LKB1 and MO25 (punctate appearance) co-localize with the Z-disk protein, alpha-actinin (phalloidin is used as an F-actin stain) in both skinned **(Figure 4; top panels**) and intact cardiomyocytes **(Figure 4; bottom panels**). The Z-disk has not only structural functions but has also become a nodal site for myocyte signaling [32]. Furthermore, the presence of the LKB1 complex in the region of the Z-disk coincides with AMPK staining [33, 34]. Our preliminary data imaging AMPK indicates a striated, punctate staining pattern at the Z-disk similar to that seen with MO25 (data not shown).

AMPK/LKB1 complex alters association with myofibrillar proteins with cellular “energy” stress

As stated previously, a proposed mechanism for regulating contractile function is through AMPK/LKB1 localization to myofilament proteins. Furthermore, changes in subcellular localization can occur by altering binding or association with other proteins. Again, this is similar to the CK phosphotransfer system where discrete, subcellular CK pools respond and redistribute to changes in energy stress. Thus, as we are seeking to understand the role of LKB1 in the heart, we hypothesized that either an increase or a decrease in cellular energy stress will impact AMPK/LKB1 myofilament localization. Accordingly, we subjected hearts to energy stress and determined the relative amount of AMPK/LKB1 complex associated with myofilament proteins. To do this, we first perfused rat hearts with a modified Krebs-Henseleit solution [27] or a modified Krebs-Henseleit mixed with 5-amino-1-β-D-ribofuranosyl-imidazole-4-carboxamide (AICAR), a cell permeable AMP mimetic to activate AMPK without affecting the intracellular AMP:ATP ratio [35]. Next, hearts were excised, minced and prepared in 2 ways: (1) tissue was mechanically disrupted and demembranated as above, or (2) subjected to a myofibrillar extraction protocol, a preparation that isolates myofibrillar proteins and separates substrates for ATP hydrolysis

from residual ATP and other cytoskeletal components [36-38]. Removal of substrate eliminates residual ATPase activity that might impact AMPK/LKB1 activity unintentionally and alter myofilament localization.

Next, we took demembranated and myofibrillar samples and immunoblotted for AMPK, phosphorylated-AMPK (pAMPKα_{T172}), MO25 and LKB1. When comparing AICAR- and control-treated hearts following demembranation, the amount of AMPK/LKB1 protein is not different (**Figure 5A**). When myofilament proteins are separated from energetic substrates (myofibrillar preparation), AICAR treatment reduces myofibrillar association with all members of the AMPK/LKB1 signaling axis (**Figure 5D**). However, AICAR acts as an AMP mimetic and activates AMPK without altering the AMP:ATP ratio [35]. Therefore, AICAR-dependent activation of AMPK in the context of "normal" levels of ATP and ADP would be more representative of a non-pathological increase in energy demand, unlike CVD.

Accordingly, we examined AMPK/LKB1-myofilament interaction in a chronic CVD setting. For these studies, we immunoblotted for AMPK/LKB1 signaling axis members in demembranated or myofibrillar samples from FHC, myosin heavy chain(MHC)-R403Q and cardiac Troponin T(cTnT)-R92Q, male hearts. These FHC models were chosen as they have established alterations in cardiac energetics [39, 40]. Mice containing the R403Q mutation have a lowered phosphocreatine to ATP ratio, and increased tension cost [41]. The R92Q mutation not only diminishes the driving force for ATPase reactions (ΔG_{ATP}), but also blunts contractile reserve [40]. In both FHC samples, like AICAR-treated samples, the amounts of AMPK/LKB1 complex proteins are not different in demembranated samples (**Figure 5B**). In contrast to AICAR treatment (**Figure 5D**), the association of AMPK, pAMPKα_{T172}, LKB1, and MO25 with myofibrillar proteins increases in both FHC models (**Figure 5E**). This increased association occurs despite our finding of an overall decrease in cellular MO25, AMPKα and pAMPKα in male MHC-R403Q hearts [42]. The bar graph (**Figure 5C,F**) summarizes the Western blot analysis.

LKB1 complex interacting proteins

If an alteration of cellular energy re-distributes members of the AMPK/LKB1 signaling axis, our next series of experiments were directed at determining *where* these proteins re-distribute. First, we used a co-immunoprecipitation (Co-IP) strategy with demembranated cardiac tissue from rat hearts treated with the GST-LKB1 complex and then added to a column coated with an anti-MO25 antibody; eluent from this column was subjected to SDS-PAGE (**Figure 6A**). Following gel extraction, LC-MS/MS identified several proteins (summarized in **Table 2**) including mitochondrial ATP Synthase (Complex V) (band 1) and NAD(P) Transhydrogenase and 2-oxogluterate dehydrogenase (band 7,8), all of which are involved in mitochondrial ATP production. Also in band 7,8 was vinculin, a cytoskeletal protein that is sensitive to myocyte loading and re-distributes in aged hearts [43]. The suggestion is that LKB1 complex proteins interact with energetic enzymes and cytoskeletal proteins.

Next, we implemented the following strategy to better understand how myofilament cellular energy impact AMPK/LKB1 localization. Again, hearts were perfused with or without AICAR and cardiac tissue was demembranated or myofibrils were prepared and subjected to

SDS-PAGE. Demembranated cardiac tissue showed a similar protein profile between control- and AICAR-treated hearts (**Figure 6B; left panel**). Myofibrillar preparations, on the other hand, highlighted key proteins that were present in control- but not AICAR-treated hearts (**Figure 6B; central panel**). Using a low-stringency Co-IP (anti-MO25 columns) strategy to capture only robust changes in protein interaction, we demonstrated that proteins absent in AICAR-treated myofibrils remained associated with the LKB1 complex following anti-MO25 Co-IP (**Figure 6B; right panel**). LC-MS/MS verified that the proteins absent in AICAR treated myofibrils but associate with the LKB1 complex were, again, vinculin (1) and mitochondrial ATP Synthase (Complex V) (2).

Discussion

Our lab has a long history in studying the impact of signaling pathways on contractile mechanisms downstream of Ca^{2+} binding to troponin C [44-46]. Several groups, including ours, have validated the significance of the AMPK signaling network as a key regulator of contractile function through post-translational modification (PTM) of cardiac troponin I (cTnI) [2-6]. The goal of this study was to gain understanding into how the upstream kinase complex, LKB1/MO25/STRAD (LKB1 complex), functions to interact with myofilament proteins and alter contractility independently of AMPK signaling, and, presumably, PTM. Emphasis was placed on how this complex interacts with myofilament proteins within the heart under both normal energy conditions, and under energy stress as a majority of energy resources are used to fuel cardiac contraction. We hypothesized that the LKB1 complex can target myofilament proteins, and that targeting or localization can change with energy status. We found that 1) the LKB1 complex decreases Ca^{2+}-sensitivity of tension development and maximum tension generation capacity, 2) myofibrillar proteins retain or bind to LKB1 and Mo25 post LKB1 complex treatment 3) altered cardiovascular energetics change binding of LKB1 and Mo25 to myofibrillar proteins and 4) the potential target of the LKB1 complex is located at the Z-Disk.

A major finding of this study was that the LKB1 complex decreases relative Ca^{2+}-sensitivity of tension and blunts maximum tension development. Interestingly, this effect of LKB1 on contractility is presumably independent of changing the rate of tension redevelopment. Using a simplified two-state, cross-bridge model, the rate of tension redevelopment is proportional to both the attachment and detachment rates, and, it is likely that LKB1 alters either attachment, detachment or both based on robust decreases in Ca^{2+}-sensitivity and maximum tension. It is also likely that the physical association of the LKB1 complex to the myofilaments may functionally interfere with the myosin ATPase in much the same way as muscle CK. It has been shown that the structural association between CK and the myofilament (at the M line) is functionally coupled to myosin ATPase such that CK limits maximum myosin ATPase [16]. Therefore, we predict that the LKB1 complex-myofilament signaling axis can potentially impact tension generation and cardiac energy reserve in the whole heart. Future studies will be directed at determining how LKB1 complex signaling impacts tension cost or efficiency of ATP use.

The exact mechanism of how the LKB1 complex alters myofilament contractile function remains unclear. In this study, we show that LKB1 complex proteins associate with

myofibrils following a stringent wash-out protocol. This could indicate a novel regulatory mechanism for the LKB1 complex in the heart. Further interrogation indicates that components of the LKB1 complex (LKB1 and MO25) co-localize at the sarcomeric Z-disk. It is now appreciated that Z-disk complex proteins not only impart structural integrity to the myocyte but also function as a nodal site for myocyte signaling [32]. Furthermore, the presence of the LKB1 complex in the region of the Z-disk coincides with AMPK staining [33, 34]. Our preliminary data (data not shown) indicates punctate staining of AMPK also at the Z-disk. Co-localization of AMPK and LKB1 complex proteins at the Z-disk is not surprising considering the ability to form an active AMPK/LKB1 signaling complex as suggested [47].

When hearts were excised and perfused with AICAR, a cell permeable AMP mimetic to activate AMPK [35], localization of LKB1 complex proteins determined by immunofluorescence is not visibly altered. Due to the intense staining at the Z-disk, subtle changes in localization are most likely masked. Therefore, we took an alternative approach in which we compared AMPK/LKB1 protein abundance in samples prepared in 2 ways (demembranated vs myofibrillar). The reason for this comparison is that cardiac tissue subjected to a myofibrillar extraction protocol isolates myofibrillar proteins and separates substrates for ATP hydrolysis from residual ATP and other cytoskeletal components [36-38]. This preparation also allows rigorous control of substrate concentration and direct assessment of myofibrillar ATPase activity. When examining cardiac tissue that was demembranated, there is no change in LKB1, MO25, AMPKα, or pAMPKα$_{172}$ abundance with AICAR administration. However, relative levels for each AMPK/LKB1 complex protein significantly decreases with AICAR treatment compared to controls.

Because AICAR acts as an AMP analogue and activates AMPK without altering cellular AMP:ATP ratio [35], AICAR treatment may be more representative of a non-pathological increase in energy demand. In contrast to AICAR treatment, the association of AMPKα, pAMPKα$_{T172}$, LKB1, and MO25 with myofibrillar preparations increases in both FHC models. This increased association occurs despite our finding of an overall decrease in cellular MO25, AMPKα and pAMPKα in male MHC-R403Q hearts [42].

Elegant studies indicate that familial hypertrophic cardiomyopathy(FHC)-causing mutations in sarcomeric proteins disturb the energetic landscape leading to cardiomyopathies [40, 48, 49]. These studies unambiguously support the notion that downstream perturbations in sarcomeric function represent the earliest indicators of pathological cardiac remodeling [1]. The suggestion is that FHC mutations, known to alter cross-bridge kinetics/energetics [40, 48-51], increase sarcomeric AMP levels and recruit AMPK/LKB1 complex proteins to sarcomeric myofibrils in an attempt to manage disturbances in cross-bridge cycling due to FHC mutations. On the other hand, increases in cellular AMP in the absence of myofibrillar dysfunction, decreases AMPK/LKB1 association with myofilament proteins. The implication is that altering cellular AMP instigates a re-distribution or subcellular localization of AMPK/LKB1 signaling complexes. There is evidence to suggest that AMP acts as a low energy signal to recruit the formation of a AMPK/LKB1 activating complex, which once formed increases AMPK activation 100 fold [22]. Coincidentally, a key

regulatory mechanism of LKB1 is altering localization or association with other proteins within the cell, especially in striated muscle where LKB1 is constitutively active [52].

We then implemented a strategy to better elucidate the mechanism of AMPK/LKB1 re-distribution following energy stress. First, we performed a Co-IP on demembranated cardiac trabeculae using anti-MO25 coated columns, as MO25 is a scaffolding protein. Followed by a stringent elution protocol, we gel-extracted several prominent proteins bands and subjected the samples to LC-MS/MS. Next, using SDS-PAGE to compare protein profiles between demembranated and myofibrillar preparations, several proteins bands were visible in control-treated compared to AICAR-treated myofibrillar samples. Using a low-stringency Co-IP (anti-MO25 columns) strategy to capture only robust changes in protein interaction, we demonstrate that proteins absent in AICAR-treated myofibrils remain associated with the LKB1 complex following anti-MO25 Co-IP. LC-MS/MS verified that the proteins absent in AICAR treated myofibrils but associate with the LKB1 complex are vinculin and mitochondrial ATP Synthase (Complex V). The suggestion is that LKB1 complex proteins interact with energetic enzymes and cytoskeletal proteins.

Although we have not validated the nature of the association, functional coupling between LKB1 complex proteins and cytoskeletal proteins such as vinculin would be predicted based on Z-disk co-localization. Vinculin is a member of a multi-protein complex linking the actin-cytoskeleton to the sarcolemma and, through interactions with integrins and cadherins, influences cell-cell or cell-matrix interactions [53]. Vinculin is sensitive to mechanical loading of cardiomyocytes, and, recently shown to re-distribute in aged rodents and simians [43]. The suggestion is that vinculin, apart from a structural and signaling role in mechano-sensing, may be sensitive to alterations in cellular energy that may be communicated through the AMPK/LKB1 signaling network. An interaction between LKB1 and ATP Synthase is more self-evident, considering that both have critical roles in energy “sensing”. To date, no functional association between the LKB1 complex and ATP Synthase has been established.

To conclude, we illustrate a novel role for the LKB1 complex as a modifier of myofilament function. The ability of LKB1 to impact contractile properties within the sarcomere is independent of AMPK signaling. Furthermore, we have demonstrated that the LKB1 complex can target myofilament proteins with predominant co-localization at the Z-disk of the cardiac myocyte. Moreover, we identify potential interacting partners whose association changes with cellular energy stress. Future work will be directed at elucidating the cellular and molecular mechanisms by which LKB1 regulates myofilament function and validating localization and protein-protein interactions.

Acknowledgements

This work was supported by National Institutes of Health grant HL098256, a National Mentored Research Science Development Award (K01 AR052840) and Independent Scientist Award (K02 HL105799) from the NIH to J.P.K., and an Interdisciplinary Training Grant in Cardiovascular Sciences (HL007249). NIH grants HL108625 and HL123078 (to C.C.G.) and HL075619 (to J.C.T) also provided support for this work. Support was also received from the Sarver Heart Center at the University of Arizona and the Steven M. Gootter Foundation. Mass spectrometry and proteomics data were acquired by the Arizona Proteomics Consortium supported by NIEHS grant ES06694 to the SWEHSC, NIH/NCI grant CA023074 to the UA Cancer Center and by the BIO5 Institute of the

University of Arizona. The Thermo Fisher LTQ Orbitrap Velos mass spectrometer was provided by grant 1S10 RR028868-01 from NIH/NCRR.

References

[1]. Yar S, Monasky MM, Solaro RJ. Pflugers Arch. 2014; 466:1189–1197. [PubMed: 24488009]

[2]. Oliveira SM, Zhang YH, Solis RS, Isackson H, Bellahcene M, Yavari A, Pinter K, Davies JK, Ge Y, Ashrafian H, Walker JW, Carling D, Watkins H, Casadei B, Redwood C. Circ Res. 2012; 110:1192–1201. [PubMed: 22456184]

[3]. Nixon BR, Thawornkaiwong A, Jin J, Brundage EA, Little SC, Davis JP, Solaro RJ, Biesiadecki BJ. J Biol Chem. 2012; 287:19136–19147. [PubMed: 22493448]

[4]. Sancho Solis R, Ge Y, Walker JW. Protein science : a publication of the Protein Society. 2011; 20:894–907. [PubMed: 21416543]

[5]. Behunin SM, Lopez-Pier MA, Birch CL, McKee LA, Danilo C, Khalpey Z, Konhilas JP. Biophys J. 2015; 108:1484–1494. [PubMed: 25809261]

[6]. Buscemi N, Foster DB, Neverova I, Van Eyk JE. Circ Res. 2002; 91:509–516. [PubMed: 12242269]

[7]. Stehle R, Iorga B. J Mol Cell Cardiol. 2010; 48:843–850. [PubMed: 20060002]

[8]. Solaro RJ, Henze M, Kobayashi T. Circ Res. 2013; 112:355–366. [PubMed: 23329791]

[9]. Ingwall JS. Cardiovasc Res. 2008

[10]. Doenst T, Nguyen TD, Abel ED. Circ Res. 2013; 113:709–724. [PubMed: 23989714]

[11]. Ingwall JS. Cardiovasc Res. 2009; 81:412–419. [PubMed: 18987051]

[12]. Neubauer S. N Engl J Med. 2007; 356:1140–1151. [PubMed: 17360992]

[13]. Ingwall JS, Shen W. Eur J Heart Fail. 2010; 12:1268–1270. [PubMed: 21098578]

[14]. Aksentijevic D, Lygate CA, Makinen K, Zervou S, Sebag-Montefiore L, Medway D, Barnes H, Schneider JE, Neubauer S. Eur J Heart Fail. 2010; 12:1282–1289. [PubMed: 20940173]

[15]. Koons S, Cooke R. Adv Exp Med Biol. 1986; 194:129–137. [PubMed: 3529853]

[16]. Ventura-Clapier R, Kuznetsov A, Veksler V, Boehm E, Anflous K. Mol Cell Biochem. 1998; 184:231–247. [PubMed: 9746324]

[17]. Dzeja P, Terzic A. International journal of molecular sciences. 2009; 10:1729–1772. [PubMed: 19468337]

[18]. Hardie DG, Hawley SA, Scott JW. J Physiol. 2006; 574:7–15. [PubMed: 16644800]

[19]. Hawley SA, Davison M, Woods A, Davies SP, Beri RK, Carling D, Hardie DG. J Biol Chem. 1996; 271:27879–27887. [PubMed: 8910387]

[20]. Suter M, Riek U, Tuerk R, Schlattner U, Wallimann T, Neumann D. J Biol Chem. 2006; 281:32207–32216. [PubMed: 16943194]

[21]. Baron SJ, Li J, Russell RR 3rd, Neumann D, Miller EJ, Tuerk R, Wallimann T, Hurley RL, Witters LA, Young LH. Circ Res. 2005; 96:337–345. [PubMed: 15653571]

[22]. Zhang YL, Guo H, Zhang CS, Lin SY, Yin Z, Peng Y, Luo H, Shi Y, Lian G, Zhang C, Li M, Ye Z, Ye J, Han J, Li P, Wu JW, Lin SC. Cell Metab. 2013; 18:546–555. [PubMed: 24093678]

[23]. Sebbagh M, Olschwang S, Santoni M-J, Borg J-P. Familial Cancer. 2011; 10:415–424. [PubMed: 21656073]

[24]. Deepa SS, Zhou L, Ryu J, Wang C, Mao X, Li C, Zhang N, Musi N, DeFronzo RA, Liu F, Dong LQ. Molecular endocrinology. 2011; 25:1773–1785. [PubMed: 21835890]

[25]. Yamada E, Pessin JE, Kurland IJ, Schwartz GJ, Bastie CC. Cell Metab. 2010; 11:113–124. [PubMed: 20142099]

[26]. Ventura-Clapier R, Kaasik A, Veksler V. Mol Cell Biochem. 2004; 256-257:29–41. [PubMed: 14977168]

[27]. Konhilas JP, Irving TC, De Tombe PP. J Physiol. 2002; 544:225–236. [PubMed: 12356894]

[28]. Layland J, Solaro RJ, Shah AM. Cardiovasc Res. 2005; 66:12–21. [PubMed: 15769444]

[29]. Nesvizhskii AI, Keller A, Kolker E, Aebersold R. Anal Chem. 2003; 75:4646–4658. [PubMed: 14632076]

[30]. Brenner B. Proc Natl Acad Sci U S A. 1988; 85:3265–3269. [PubMed: 2966401]

[31]. Cuello F, Bardswell SC, Haworth RS, Ehler E, Sadayappan S, Kentish JC, Avkiran M. J Biol Chem. 2011; 286:5300–5310. [PubMed: 21148481]

[32]. Frank D, Frey N. J Biol Chem. 2011; 286:9897–9904. [PubMed: 21257757]

[33]. Pinter K, Grignani RT, Watkins H, Redwood C. J Muscle Res Cell Motil. 2013; 34:369–378. [PubMed: 24037260]

[34]. Gregor M, Zeold A, Oehler S, Marobela KA, Fuchs P, Weigel G, Hardie DG, Wiche G. J Cell Sci. 2006; 119:1864–1875. [PubMed: 16608880]

[35]. Sun Y, Connors KE, Yang DQ. Mol Cell Biochem. 2007; 306:239–245. [PubMed: 17786544]

[36]. Chandra M, Montgomery DE, Kim JJ, Solaro RJ. J Mol Cell Cardiol. 1999; 31:867–880. [PubMed: 10329214]

[37]. Solaro RJ, Wise RM, Shiner JS, Briggs FN. Circ Res. 1974; 34:525–530. [PubMed: 4275030]

[38]. Brown A, Aras A, Hass GM. J Biol Chem. 1959; 234:438–440. [PubMed: 13630926]

[39]. Spindler M, Saupe KW, Christe ME, Sweeney HL, Seidman CE, Seidman JG, Ingwall JS. J Clin Invest. 1998; 101:1775–1783. [PubMed: 9541509]

[40]. Javadpour MM, Tardiff JC, Pinz I, Ingwall JS. J Clin Invest. 2003; 112:768–775. [PubMed: 12952925]

[41]. Witjas-Paalberends ER, Ferrara C, Scellini B, Piroddi N, Montag J, Tesi C, Stienen GJ, Michels M, Ho CY, Kraft T, Poggesi C, van der Velden J. J Physiol. 2014; 592:3257–3272. [PubMed: 24928957]

[42]. Chen H, Untiveros GM, McKee LA, Perez J, Li J, Antin PB, Konhilas JP. PLoS ONE. 2012; 7:e41574. [PubMed: 22844503]

[43]. Kaushik G, Spenlehauer A, Sessions AO, Trujillo AS, Fuhrmann A, Fu Z, Venkatraman V, Pohl D, Tuler J, Wang M, Lakatta EG, Ocorr K, Bodmer R, Bernstein SI, Van Eyk JE, Cammarato A, Engler AJ. Sci Transl Med. 2015; 7:292ra299.

[44]. Konhilas JP, Irving TC, Wolska B, Martin AF, Solaro RJ, de Tombe PP. Circulation. 2000; 102:II–215.

[45]. Solaro RJ, Moir AJG, Perry SV. Nature. 1976; 262:615–617. [PubMed: 958429]

[46]. de Tombe PP, Stienen GJ. Circ Res. 1995; 76:734–741. [PubMed: 7728989]

[47]. Hardie DG. Cell Metabolism. 2014; 20:939–952. [PubMed: 25448702]

[48]. Ford SJ, Mamidi R, Jimenez J, Tardiff JC, Chandra M. J Mol Cell Cardiol. 2012; 53:542–551. [PubMed: 22884844]

[49]. Chandra M, Tschirgi ML, Tardiff JC. Am J Physiol Heart Circ Physiol. 2005; 289:H2112–2119. [PubMed: 15994854]

[50]. Palmiter KA, Tyska MJ, Haeberle JR, Alpert NR, Fananapazir L, Warshaw DM. J Muscle Res Cell Motil. 2000; 21:609–620. [PubMed: 11227787]

[51]. Tyska MJ, Hayes E, Giewat M, Seidman CE, Seidman JG, Warshaw DM. Circ Res. 2000; 86:737–744. [PubMed: 10764406]

[52]. Sakamoto K, Goransson O, Hardie DG, Alessi DR. Am J Physiol Endocrinol Metab. 2004; 287:E310–317. [PubMed: 15068958]

[53]. Zemljic-Harpf A, Manso AM, Ross RS. Journal of investigative medicine : the official publication of the American Federation for Clinical Research. 2009; 57:849–855. [PubMed: 19952892]

Highlights

- The upstream AMP-activated kinase (AMPK) complex, LKB1/MO25/STRAD, decreases myofilament Ca^{2+}-sensitivity and blunts maximum tension
- LKB1/MO25/STRAD complex associates with myofibril proteins
- LKB1/MO25/STRAD complex co-localizes with the Z-disk of the cardiac sarcomere
- AMPK/LKB1 complex re-distributes with energy stress

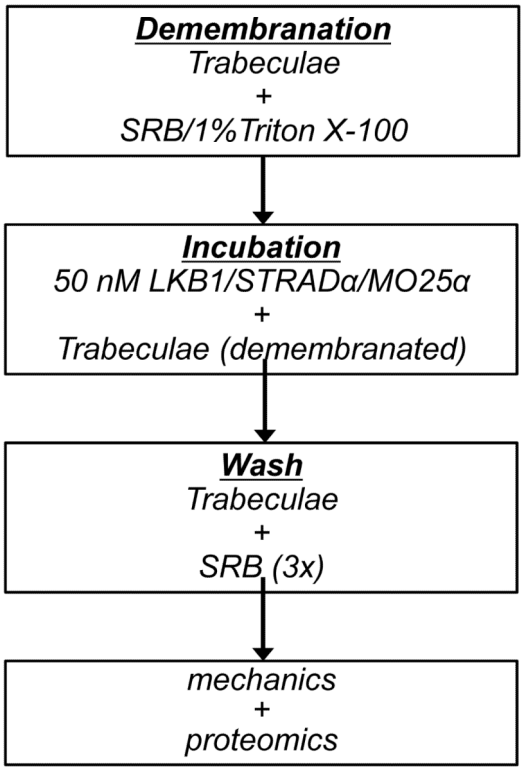

Figure 1. Treatment protocol for LKB1 targeting of myofilament proteins

Rat cardiac trabeculae were excised and demembranated in standard relaxing solution (SRB) containing 1% Triton X-100. Next, trabeculae were incubated with LKB1 holoenzyme (LKB1/MO25/STRAD). Finally, trabeculae were washed 3x for 15 minutes each wash prior to use in myofilament mechanics or proteomic analysis.

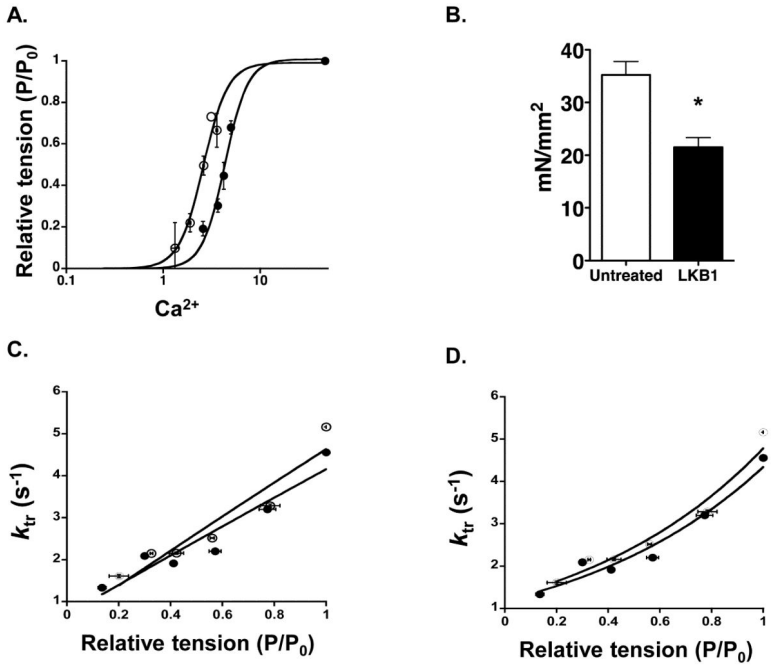

Figure 2. Myofilament mechanics in untreated and treated demembranated cardiac trabeculae

(A) Ca^{2+}-sensitivity of tension in trabeculae treated with the LKB1 complex (closed circles) compared to untreated fibers (open circles). Sarcomere length was set to 2.2μm and all data were normalized to saturating Ca^{2+} (maximal) tension. **(B)** Tension development at maximum activating Ca^{2+} in trabeculae treated (closed circles) or untreated (open circles) with the LKB1 complex. **(C)** and **(D)** The rate constant for tension redevelopment (k_{tr}) was plotted against relative force and fit by a linear (**C**) or curvilinear (**D**) model in trabeculae treated (closed circles) or untreated (open circles) with the LKB1 complex. Sample size and statistical analysis detailed in Table 1.

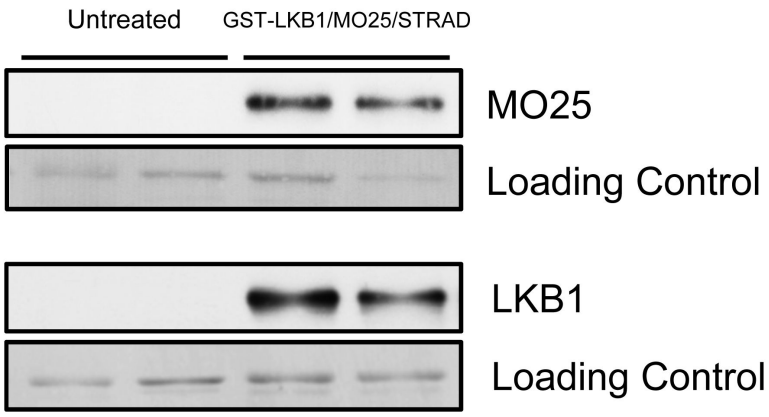

Figure 3. Western blot of GST-LKB1/MO25/STRAD treated myofibrils

Myofibrils isolated from untreated demembranated cardiac trabeculae and trabeculae treated with recombinant GST fused LKB1/MO25/STRAD were probed for MO25 and LKB1. Myofibrils exposed to GST-LKB1/MO25/STRAD retained the LKB1 complex post washout.

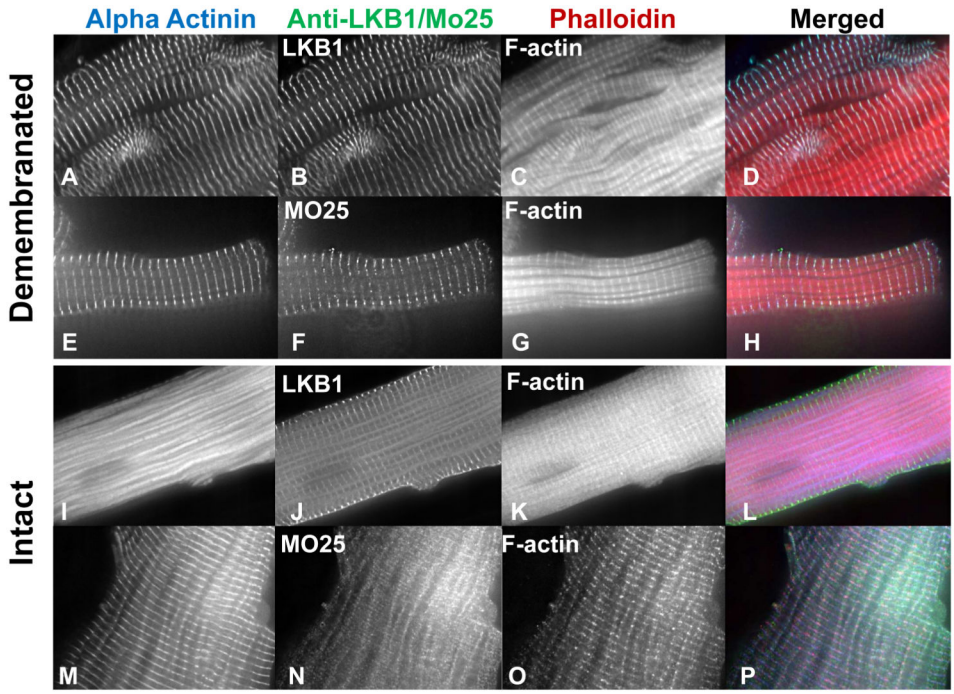

Figure 4. Immunofluorescent staining of demembranated and membrane-intact cardiomyocytes

Cardiac myocytes were isolated and prepared for immunohistochemistry using fluorescently labeled antibodies to LKB1 and MO25 in demembranated (**A-H**) and membrane intact (**I-P**) cardiomyocytes. Staining indicated by arrows is detailed as follows: Alpha-actinin, Z-disk protein (**A,E,I,M**); LKB1 (**B,J**); MO25 (**F,N**); Phalloidin, F-actin (**C,G,K,O**). Merged panels show co-localization of LKB1 (**D,L**) or MO25 (**H,P**) with alpha-actinin and phalloidin.

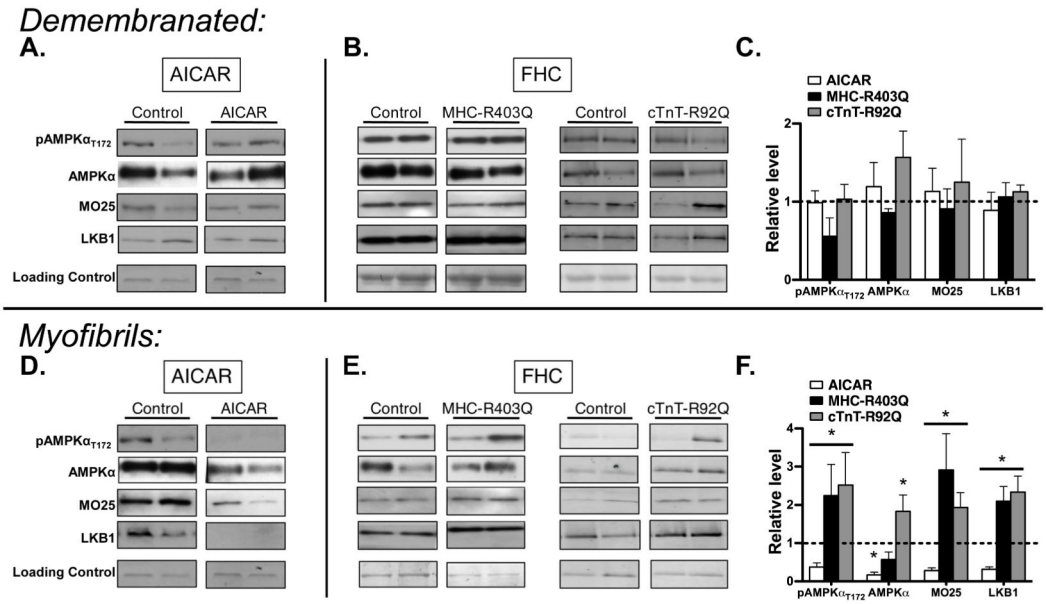

Figure 5. Impact of energy stress on myofibril-AMPK/LKB1 interaction

Western blot analysis of demembranated cardiac trabeculae or cardiac myofibrils. Demembranated (**top panels; A,B**) and myofibrillar fractions (**bottom panel; D,E**) from AICAR perfused (**left panels; A,D**) or familial hypertrophic cardiomyopathy (FHC; **right panels; B,E**) hearts were immunoblotted for pAMPKα$_{172}$, AMPKα, MO25, and LKB1. **C,F**: Bar graph summary of relative protein levels compared to controls from demembranated (**C**) and myofibrillar (**F**) experimental groups. (n=5 per group *p<0.05 from control groups represented by dotted line).

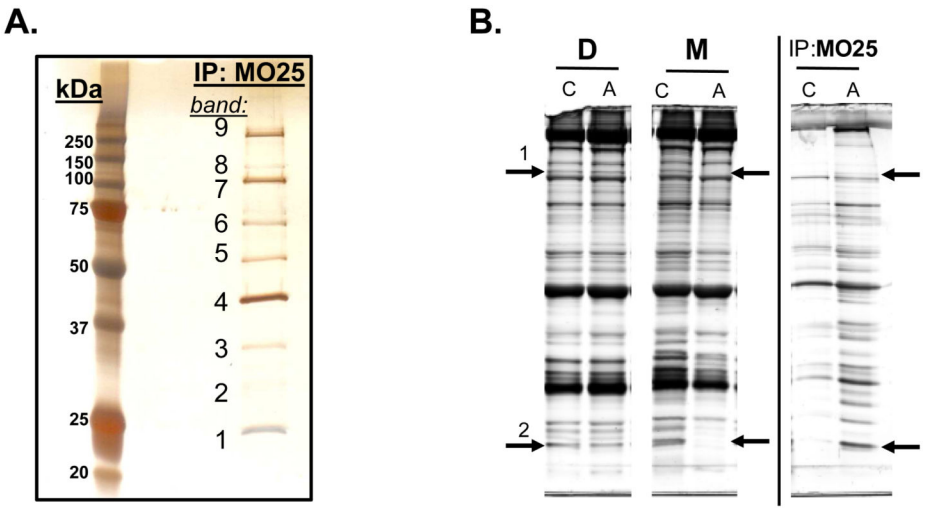

Figure 6. Co-Immunoprecipitation of untreated and AICAR-treated rat hearts

(**A**) Demembranated cardiac tissue treated with the LKB1 complex was added to a column containing anti-MO25 antibodies. After a stringent elution protocol, eluent was subjected to SDS-PAGE. Bands 1 and 7-8 were analyzed by LC/MS/MS and detailed in Table 2. (**B**) Hearts were perfused with Krebs-Henseleit containing 2mM AICAR (lanes labeled **A**) or hearts perfused with control (no AICAR) Krebs-Henseleit (lanes labeled **C**). Next, SDS-PAGE was used to separate demembranated samples (labeled **D, 2 left bands**) or myofibril samples (labeled **M, 2 middle bands**) prepared from AICAR- or control-perfused hearts. Co-Immunoprecipitation using AICAR- or control-perfused hearts (lanes labeled **IP: MO25**) with anti-Mo25 immobilized on the column followed by silver stain revealed a unique banding pattern. Arrows highlight proteins/bands absent in myofibril, AICAR treated samples but present in MO25 Co-IP preparations. LC/MS/MS identified bands labeled 1 and 2.

Table 1

Mean Values for Hill Fit to Ca^{2+}-Tension Curve.

Table 1A. ***Ca^{2+}-Sensitivity of Tension Development***		
	Untreated (n)	**LKB1 Complex Treated (n)**
EC_50 (μM)	3.23±0.25 (14)	5.00±0.52 * (11)
pCa_{50}	5.50±0.03 (14)	5.31±0.04 * (11)
Hill Coefficient	3.93±0.30 (14)	3.75±0.54 (11)
Maximum Tension (mN/mm^2)	35.22±2.58 † (21)	21.50±1.83 * (17)
Table 1B. ***Rate Constant for Tension Redevelopment***		
k_{tr} Max (s^{-1})	5.16±0.37 (8)	4.56±0.34 (8)
Linear fit ($s^{-1}/P/P_0$)	5.78±0.48 (8)	5.46±0.37 (8)

Each column contains mean values ± standard error for the Ca^{2+}-tension relationship in rat cardiac trabeculae that were either untreated or treated with exogenous LKB1 complex. Sarcomere length was set to 2.2μm. Ca^{2+}-sensitivity of tension for each group is indicated by EC_{50} (μM) and pCa_{50}. There is a decrease Ca^{2+}-sensitivity in fibers treated with LKB1 complex alone ($p<0.05$). There was no statistical difference in cooperativity (Hill Coefficient). Maximum tension generation was also determined; there is a decrease in total tension generation in fibers that were treated with the LKB1 complex. The rate constant for tension redevelopment at maximum tension was not different between untreated and treated groups; the relationship between relative force (P/P_0) and $\mathbf{k_{tr}}$ was not different between experimental groups studied.

* ($p<0.05$).

Table 2

LC-MS/MS of Mo25 Coupled Co-IP, LKB1 Complex Treated Tissue.

Band 7-8	Vinculin	**117 kDa**
	2-oxogluterate dehydrogenase	**116 kDa**
	SERCA2a	**115 kDa**
	NAD (P) Transhydrogenase	**114 kDa**
	Alpha Actinin 2	**104 kDa**
	Catenin, Alpha	**100 kDa**
	Catenin, Beta-1	**85 kDa**
	Junction Plakoglobin	**82 kDa**
Band 1	ATP Synthase Subunit O (Complex V)	**24 kDa**
	Myosin Light Chain 3	**22 kDa**

Protein identification of bands 1, 7, and 8 (**Figure 6A**) that meet the requirements of over a 99.0% protein threshold and at least 2 unique peptides; this selection criteria gives an effective false detection rate of 0%. Protein identification must also be in the correct molecular weight range for the selected band. Proteins are listed by closest in molecular weight to the standard marker used.